SPANDIDOS PUBLICATIONS

ONCOLOGY LETTERS 16: 7231-7238, 2018

FK866 inhibits the epithelial-mesenchymal transition of hepatocarcinoma MHCC97-H cells

BIN ZHANG[1,2], DONGMEI SHI[3], XIANGYU ZHANG[4], GUANZHAO LIANG[5], WEIDA LIU[5] and SEN QIAO[2]

[1]School of Medicine and Life Sciences, University of Jinan-Shandong Academy of Medical Sciences, Jinan, Shandong 250062; Departments of [2]Hepatobiliary Surgery, [3]Dermatology and [4]Pathology, Jining No. 1 People's Hospital, Jining, Shandong 272011; [5]Department of Mycology, Institute of Dermatology, Chinese Academy of Medical Sciences, Peking Union Medical College, Nanjing, Jiangsu 210042, P.R. China

Received February 23, 2018; Accepted September 26, 2018

DOI: 10.3892/ol.2018.9541

Abstract. Epithelial-mesenchymal transition (EMT) is known to serve a pivotal function in hepatocellular carcinoma (HCC) metastasis. Nicotinamide phosphoribosyltransferase (NAMPT), the key enzyme in the nicotinamide-adenine dinucleotide (NAD^+)-mediated pathway for the activation of silent information regulator 1 (SIRT1), serves a key function in HCC cell invasion and metastasis. Previous studies demonstrated that FK866, a targeted NAMPT inhibitor, inhibits the viability of HCC cells and induces cancer cell apoptosis; however, the effect of FK866 on the invasion and metastasis of HCC cells, particularly those associated with EMT through the SIRT1 pathway, remains unknown. In the present study, FK866 was identified to inhibit the capability of invasion and metastasis of cells from the HCC MHCC97-H line in a dose-dependent manner using a wound healing assay, an invasion assay and a migration assay. Furthermore, FK866 markedly decreased NAD^+ and adenosine 5'-triphosphate content in MHCC97-H cells by inhibiting NAMPT expression. The results of the present study also revealed that FK866 led to a decrease in the expression of SIRT1, and to increased and decreased levels of the EMT marker proteins epithelial cadherin and vimentin, respectively, in MHCC97-H cells. Furthermore, FK866 inhibited the SIRT1-mediated EMT, invasion and migration of HCC cells by decreasing the expression of the NAMPT/NAD^+ pathway. Taken together, the results of the present study suggest that FK866 may be an effective drug targeting HCC metastasis and invasion, and that the NAMPT/NAD^+/SIRT1 pathway may be a potential therapeutic target for HCC.

Correspondence to: Professor Sen Qiao, Department of Hepatobiliary Surgery, Jining No. 1 People's Hospital, 6 Jiankang Road, Jining, Shandong 272011, P.R. China
E-mail: qsenqiao@sina.com

Key words: hepatocellular carcinoma, FK866, epithelial-mesenchymal transition, invasion, metastasis

Introduction

Hepatocellular carcinoma (HCC) is the second leading cause of cancer-associated mortality worldwide, although the survival rate of patients with HCC has improved due to curative treatments, including surgical techniques, perioperative management and a targeted drug (sorafenib) (1). However, long-term survival following surgical resection remains difficult to achieve owing to the high rate of cancer cell invasion and metastasis (2). The epithelial-mesenchymal transition (EMT) is a complex cellular process, and may be one of the underlying molecular mechanisms for enabling cancer cell invasion and metastasis, which are considered to be malignant phases of tumor progression. Furthermore, EMT has been widely reported to serve a central function in the process of HCC metastasis (3). Therefore, the development of novel agents targeting the EMT in HCC is an urgent requirement.

Silent information regulator 1 (SIRT1), a member of the mammalian sirtuin family (SIRT1-SIRT7), is involved in numerous biological processes, including drug resistance, aging, apoptosis, and tumor development and progression (4-8). Notably, previous studies have revealed that SIRT1 is associated with the EMT of HCC. The overexpression of SIRT1, which is frequently detected in human HCC specimens, promotes HCC metastasis through the EMT (9,10). SIRT1 has been proposed as a key regulator of cancer metastasis by promoting EMT. As SIRT1 is a nicotinamide-adenine dinucleotide (NAD^+)-dependent histone deacetylase, the abundance of NAD^+ directly regulates the activity of SIRT1 (11). Nicotinamide phosphoribosyltransferase (NAMPT) is the rate-limiting enzyme in the synthesis of NAD^+ via a salvage pathway (12); its expression directly determines NAD^+ levels (13). Thus, the NAMPT/NAD^+/SIRT1 pathway may be a potential alternative target in the treatment of HCC.

Previous studies have identified that FK866, a novel small-molecule NAMPT inhibitor, possesses an anticancer function in numerous types of cancer, including colon cancer, HCC, breast cancer, Ewing sarcoma, lung cancer and pancreatic cancer (12,14-18). FK866 markedly decreases the NAMPT activity and NAD^+ content in HCC cells and leads to the decrease of adenosine 5'-triphosphate (ATP) levels, which is associated with an increased rate of cell death (14).

The inhibitory effects of FK866 on NAD^+ and ATP activity, and NAD^+/SIRT1 signaling, have been well-studied and reported (19-21). However, to the best of our knowledge, the effect of FK866 on the invasion and metastasis of HCC cells, in particular through regulating the NAMPT/NAD^+/SIRT1 pathway, has not yet been reported.

The aim of the present study was to investigate whether FK866 inhibited the EMT, migration and invasion of HCC cells by mediating the NAMPT/NAD^+ signaling pathway. The inhibition of the viability of HCC cell line MHCC97-H by FK866 through the decrease in NAMPT activity and NAD^+ levels was demonstrated. Furthermore, the FK866-induced suppression of the SIRT1 expression and metastatic capability of MHCC97-H cells via the NAMPT/NAD^+ pathway was revealed, as well as the decrease in vimentin levels and increase in epithelial (E-)cadherin levels. These results indicate that the NAMPT/NAD^+/SIRT1 pathway may be a potential alternative therapeutic target and that FK866 may be an effective drug targeting HCC metastasis and invasion.

Materials and methods

Cells and treatments. The human liver tumor cell line MHCC97-H was obtained from Shanghai Zhong Qiao Xin Zhou Biotechnology Co., Ltd. (Shanghai, China) and maintained in Dulbecco's modified Eagle's medium (DMEM; Gibco; Thermo Fisher Scientific, Inc., Waltham, MA, USA) containing 10% fetal bovine serum (FBS; Excell Biology, Inc., Shanghai, China), penicillin (100 U/ml) and streptomycin (100 μg/ml) (Gibco; Thermo Fisher Scientific, Inc.) under 95% air and 5% CO_2 at 37˚C. For cell treatments, MHCC97-H cells were cultured and treated with FK866 (Beyotime Institute of Biotechnology; Shanghai, China) at concentrations of 0, 1.25, 2.5, 5, 10, 20 and 40 nM.

Cell Counting Kit-8 (CCK-8) assay. In total, ~$5x10^3$ cells/well were seeded into 96-well plates (Corning Life Sciences Inc., Midland, MI, USA) and treated with various concentrations of FK866 (0, 1.25, 2.5, 5, 10, 20 and 40 nM). Following incubation for 24, 48 and 72 h at 37˚C, CCK-8 (5 mg/ml; Sigma-Aldrich; Merck KGaA, Darmstadt, Germany) was added to each well and cells were incubated for an additional 1 h. Subsequently, the absorbance of the colored product was measured at 450 nm using a plate reader (Molecular Devices, LLC, Sunnyvale, CA, USA). Each experiment was performed at least three times.

NAD^+ assay. Total cellular NAD^+ was measured using a Microdetermination assay kit (Beijing Solarbio Science & Technology Co., Ltd., Beijing, China). In total, $5x10^6$ cells were seeded in a cell culture bottle and treated with various concentrations of FK866 (0, 2.5, 5 and 10 nM) for 24 h at 37˚C. Following the addition of 1 ml alkaline extract (Beijing Solarbio Science & Technology, Co., Ltd., Beijing, China) the mixture was ultrasonicated for 1 min and heated at 95˚C for 5 min in a water bath. From the mixture, 500 μl supernatant was collected and centrifuged at 10,000 x g for 10 min at 4˚C. Subsequently, 500 μl acid extract was added to the supernatant of the previous centrifugation and centrifuged at 10,000 x g for 10 min at 4˚C; then extracted the supernatant and preserved on ice. Of this supernatant, 200 μl was used for downstream procedures according to the protocol for the NAD^+ detection kit, using microdetermination. The absorbance was measured at 570 nm using a plate reader and the concentration of NAD^+ was determined.

ATP measurement. Total cellular ATP levels were measured using the Microdetermination assay kit. In total, $5x10^6$ cells were seeded and treated with various concentrations of FK866 (0, 2.5, 5 and 10 nM) for 24 h at 37˚C. Following the addition of 1 ml acid extract, cells were ultrasonicated for 1 min and 500 μl supernatant was collected and centrifuged at 8,000 x g for 10 min at 4˚C. Subsequently, 500 μl alkaline extract was added to the supernatant of the previous centrifugation, the mixture was centrifuged at 8,000 x g for 10 min at 4˚C, and the supernatant was preserved on ice. Finally, 200 μl supernatant was used for downstream microdetermination experiments using the ATP detection kit. According to the manufacturer's protocol, the absorbance was measured at 700 nm using a plate reader and the concentration of ATP was determined accordingly.

Wound healing assay. In total, $1x10^6$ cells were seeded into 6-well plates (Corning Life Sciences, Inc.) and incubated at 37˚C until the cells reached a confluence of ≥90%. A scratch was created using a sterile 10-μl pipette tip. Subsequently, the cells were treated with various concentrations of FK866 (0, 2.5, 5 and 10 nM) for 24 h at 37˚C. Images were acquired at 0 h and 24 h using an inverted light microscope (CKX41; Olympus Corporation, Tokyo, Japan). Thus, relative migration distance=(the gap at 0 h - the gap at 24 h)/the gap at 0 h. Cell healing and migration was observed by comparing the relative migration distance of cells treated with different concentrations of FK866 (0 and 10 nM) for 24 h.

Cell migration assay. In total, $2x10^4$ cells were plated in 200 μl DMEM without serum and containing different concentrations of FK866 (0, 2.5, 5 and 10 nM) in the upper chamber of a Transwell chamber (Corning Life Sciences, Inc.). A 500 μl volume of DMEM containing 20% FBS and similar concentrations of FK866 were added to the lower chamber, and the cells were incubated for 24 h at 37˚C. Subsequently, the cells on the upper surface of the membrane were removed using a cotton swab. The cells that migrated through the pores to the lower surface of the filter were fixed in 4% formaldehyde for 20 min and stained with 0.1% crystal violet dye for 20 min at 20˚C. Following staining, the cells were washed three times with PBS (Sigma-Aldrich; Merck KGaA). The outside membrane cells were observed at x200 magnification using an upright light microscope (Eclipse 80i; Nikon Corporation, Tokyo, Japan) and 5 fields were randomly selected to calculate an average cell count. This procedure was performed three times.

Transwell invasion assay. Matrigel invasion chambers installed with an 8.0 μm polyethylene terephthalate membrane in 24-well plates (Corning Life Sciences, Inc.) were used. In total, $5x10^4$ cells in 200 μl DMEM without serum were plated in each upper chamber, and 500 μl DMEM containing 20% FBS was added to the lower chamber as a chemoattractant; the

upper and lower chambers contained similar concentrations of FK866 (0, 2.5, 5 and 10 nM). After 24 h of conventional incubation at 37˚C, the cells on the upper surface were wiped with a cotton swab. The cells that invaded through the Matrigel and pores to the lower surface of the filter were fixed in 4% formaldehyde for 20 min and stained with 0.1% crystal violet for 20 min at 20˚C, and then washed three times with PBS. The outside membrane cells were observed at x200 magnification using an upright light microscope and 5 fields were selected randomly to calculate an average cell count. This procedure was performed three times.

Western blot analysis. In total, 5x10^6 cells were seeded in a cell culture bottle and treated with various concentrations of FK866 (0, 2.5, 5 and 10 nM) for 24 h at 37˚C. All cells were washed three times (5 min each) with ice-cold PBS and MHCC97-H cells suspended in radioimmunoprecipitation assay lysis buffer (50 mM Tris/HCl, pH 7.4, 2 mM EDTA, 1 mM dithiothreitol and 150 mM NaCl), containing 1% protease inhibitor cocktail (Thermo Fisher Scientific, Inc.), followed by centrifugation at 12,000 x g for 5 min at 4˚C to remove the cellular debris. Protein concentrations were determined using the enhanced Bincinchoninic Acid Protein assay kit (Pierce; Thermo Fisher Scientific, Inc.) according to the manufacturer's protocol. An equivalent of 50 μg protein extract was separated by SDS-PAGE (10% gel) and transferred onto polyvinylidene fluoride membranes (EMD Millipore, Billerica, MA, USA). The membranes were blocked in Tris-buffered saline with 0.1% Tween-20 containing 5% non-fat milk for 1 h at room temperature. Subsequently, the membranes were probed with the primary antibodies anti-E-cadherin (mouse; dilution, 1:1,000; cat. no. ab1416; Abcam, Cambridge, UK), anti-SIRT1 (rabbit; dilution, 1:1,000; cat. no ab32441; Abcam) and anti-vimentin (rabbit; dilution, 1:1,000; cat. no. ab92547; Abcam) at 4˚C overnight, and detected using appropriate horseradish peroxidase-conjugated secondary antibody (Goat anti-rabbit; dilution, 1:2,000. no. ab97051; Abcam) and enhanced chemiluminescence reagent (Pierce; Thermo Fisher Scientific, Inc.). The expression level of the proteins was normalized to that of GAPDH (dilution, 1:1,000; cat. no. ab9485; Abcam), which served as an endogenous control. Western blots were subjected to densitometric analysis using Quantity One software (version 4.6.2; Bio-Rad Laboratories, Inc., Hercules, CA, USA).

Statistical analysis. Statistical analyses were performed using GraphPad Prism 5 software (version 6.02; GraphPad Software, La Jolla, CA, USA). Data from 3 independent experiments were expressed as the mean ± standard deviation. Statistical significance between the groups was determined using one-way analysis of variance, followed by Student-Newman-Keuls analyses. P<0.05 for a two-tailed test was considered to indicate a statistically significant difference.

Results

FK866 inhibits the viability of the HCC cell line MHCC97-H. As a targeted NAMPT inhibitor, FK866 inhibits the viability of the HCC cells and induces cancer cell apoptosis (14). In the present study, the effects of FK866 on HCC cell viability were investigated, using the highly metastatic human MHCC97-H cell line. The inhibitory effects of FK866 on the cell viability of MHCC97-H cells were observed using the CCK-8 cell viability assay. Following incubation for various durations (24, 48 and 72 h), the cell viability was determined by measuring the absorbance at 450 nm. No significant difference was observed among the FK866-untreated group and the FK866-treated groups at lower concentrations (1.25 and 2.5 nM). Compared with the FK866-untreated group, FK866 at medium and high doses (5, 10, 20 and 40 nM) suppressed the cell viability significantly. However, no significant difference was observed among the FK866-treated groups at medium (10 nM) and high doses (20 and 40 nM). We also think that high concentration of FK866 has a greater toxic effect on normal cells; so, we screened a more reasonable range of drug concentration (0, 2.5, 5 and 10 nM) for subsequent experiments. Furthermore, no significant difference was detected in the level of cell viability using the CCK-8 assay at various time points (24-72 h). The data suggest that FK866 inhibits the viability of MHCC97-H cells in a dose-dependent, but not a time-dependent, manner (Fig. 1).

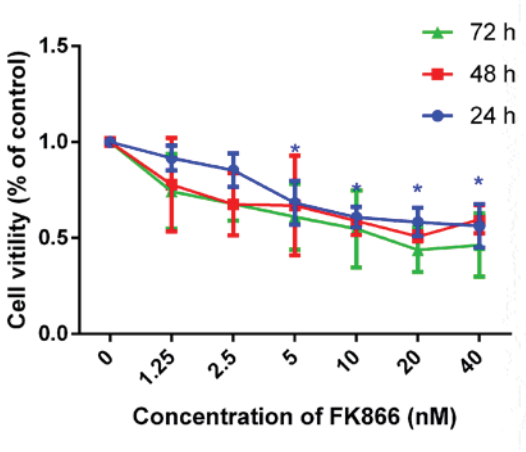

Figure 1. Inhibitory effects of FK866 on MHCC97-H cells as demonstrated using a Cell Counting Kit-8 assay. Cells were treated with various concentrations of FK866 (0-40 nM) for 24, 48 and 72 h. The cell viability is represented as the percentage cell count relative to the control as the mean ± standard error of the mean of 5 replicates in 3 separate experiments. *P<0.05.

FK866 decreases the levels of NAD$^+$ and ATP in MHCC97-H cells. NAD$^+$ is the reaction substrate of ATP and is predominantly synthesized via the salvage pathway in normal and tumor cells. NAMPT is the rate-limiting enzyme in the salvage pathway, affecting the synthesis rate and NAD$^+$ level (20). It was hypothesized that FK866 suppresses the viability of MHCC97-H cells by inhibiting NAMPT and decreasing the levels of NAD$^+$ and ATP. Therefore, various concentrations of FK866 (0, 2.5, 5 and 10 nM) were added to the cells for 24 h. Compared with the FK886-untreated group, the levels of ATP and NAD$^+$ in all the FK866-treated groups (2.5, 5 and 10 nM) were significantly lower (P<0.05), as presented in Fig. 2. Furthermore, it was identified that FK866 led to the decrease in NAD$^+$ and ATP levels in a dose-dependent manner. At the highest concentration of FK866, the levels of NAD$^+$ and ATP were at their lowest. These results suggest that FK886

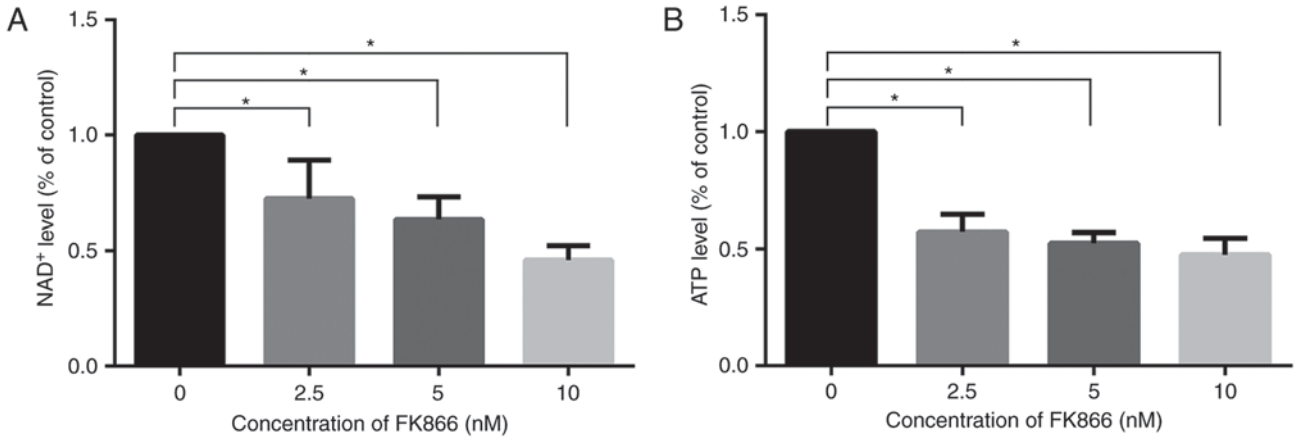

Figure 2. FK866 decreased the levels of NAD^+ and ATP. MHCC97-H cells were treated for 24 h with various concentrations of FK866 (0, 2.5, 5 and 10 nM) and the cells were collected to determine the levels of NAD^+ and ATP. (A) FK866 significantly decreased the NAD^+ level. (B) FK866 significantly decreased the ATP level. The levels of NAD^+ and ATP are expressed relative to the control as the mean ± standard error from 6 replicates of 3 separate experiments. *P<0.05. NAD, nicotinamide-adenine dinucleotide; ATP, adenosine 5'-triphosphate.

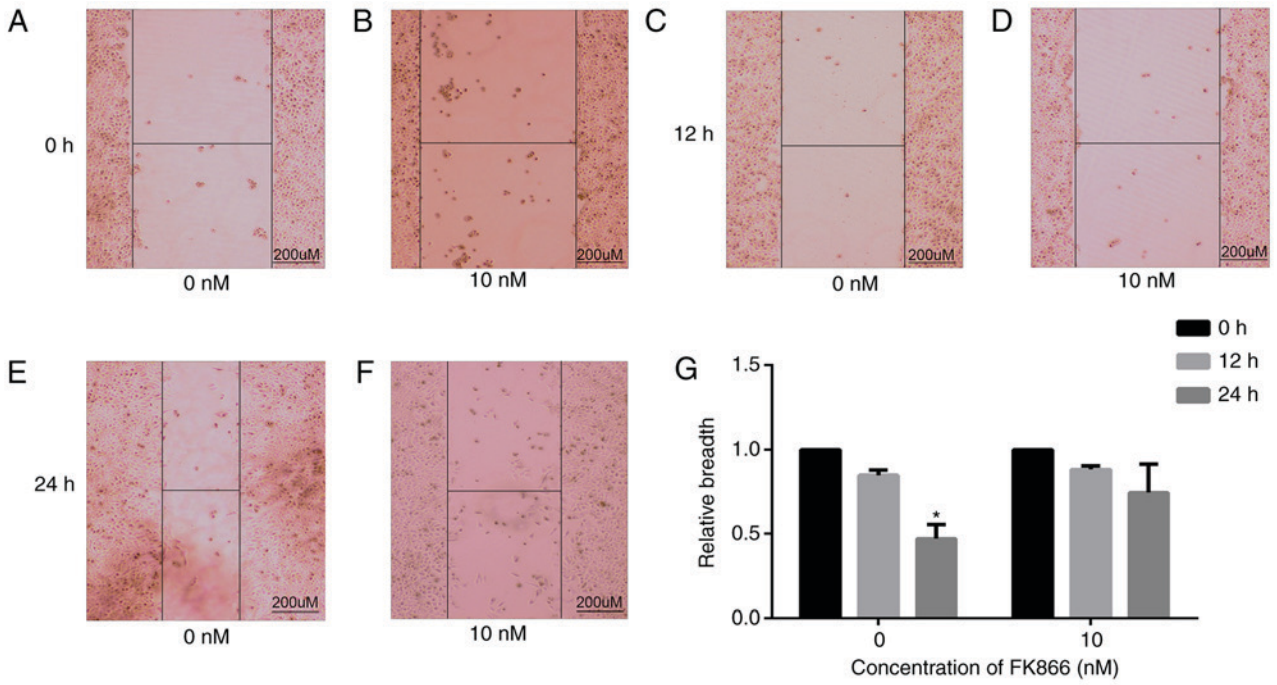

Figure 3. FK866 inhibits the healing ability of MHCC97-H cells in a concentration-dependent manner. Images of (A) control cells and (B) cells treated with 10 nM FK866 at 0 h; (C) control and (D) treated cells at 12 h; and (E) control cells and (F) treated cells at 24 h post-scratch. Scale bars, 200 μm. (G) The breadth of the wound at the initial time point (0 h) was normalized to 1 and measurements at 12 and 24 h were made relative to the initial time point. The values of the bars are the mean of 6 replicates in 3 separate experiments. The error bars represent the mean ± standard error of the mean of 6 replicates in 3 separate experiments. *P<0.05.

decreases the NAMPT activity, which causes a decline in the levels of NAD^+ and ATP in MHCC97-H cells.

FK866 inhibits the invasion and migration of MHCC97-H cells. The effects of FK866 on the invasion and metastasis of MHCC97-H cells were investigated using wound healing, invasion and migration assays. MHCC97-H cells were treated with FK866 (10 nM) and those untreated served as a negative control. After 24 h, the wound closures of control group were significantly decreased (P<0.05) compared with those at 0 h; however, the wound closures of FK866 (10 nM)-treated cells were not significantly decreased compared with those at 0 h (Fig. 3) (FK866 at 2.5 and 5 nM did not exhibit a significant effect compared with the control group; therefore, we chose two groups (0 and 10 nM) with significant differences in the results). This indicates that FK866 inhibits the healing ability of MHCC97-H cells. The migratory and invasive capabilities of MHCC97-H cells were measured using Transwell assays. The number of cells invading into the lower chambers was significantly lower upon treatment with FK866 for 24 h compared with those in the vehicle-treated control group and the decrease occurred in a concentration-dependent manner

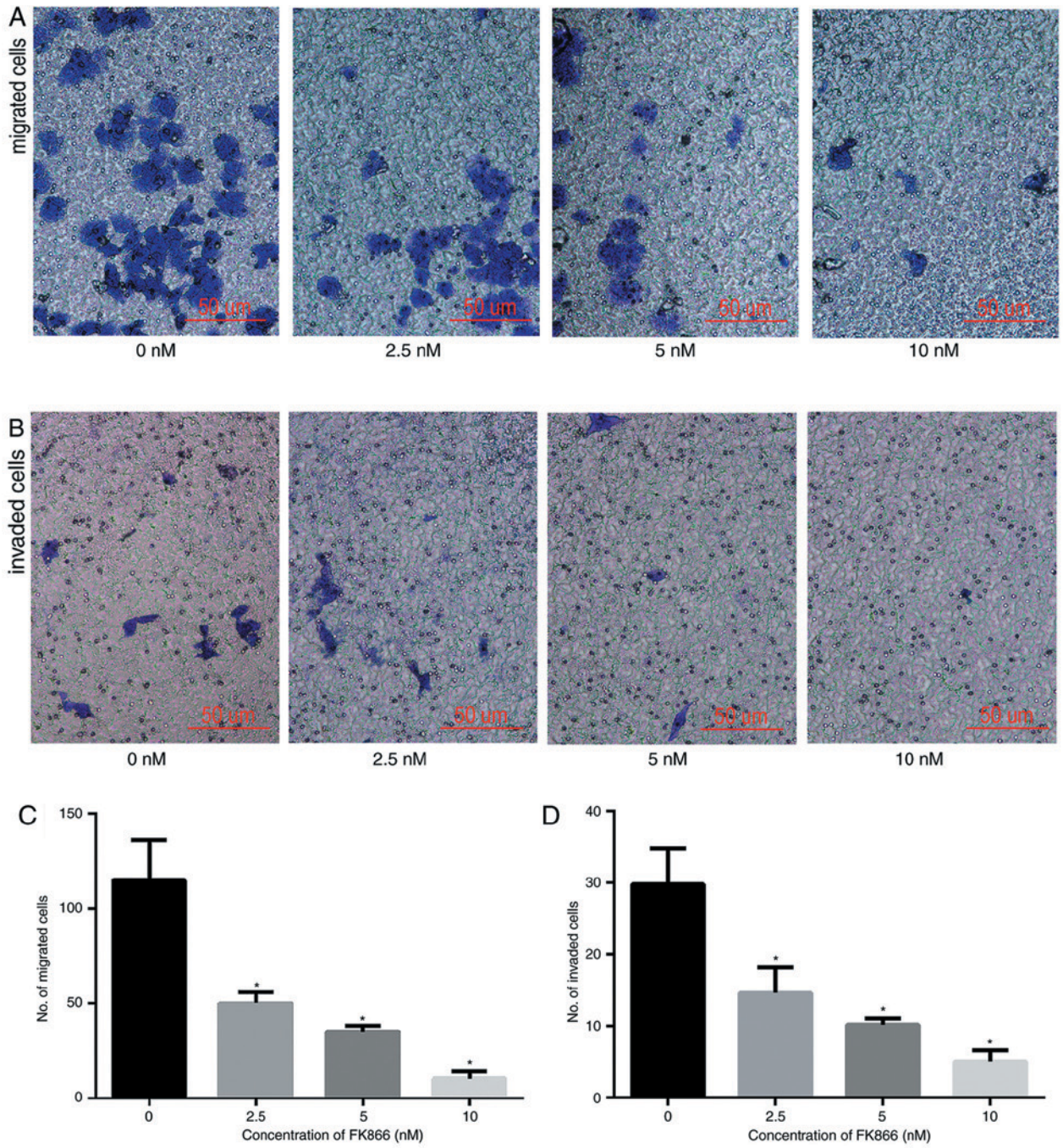

Figure 4. FK866 inhibits MHCC97-H cell invasion and migration. Transwell assays were performed in a chamber (A) without or (B) with Matrigel coating to analyze the effect of FK866 on the migration or invasion of MHCC97-H cells. FK866 (0, 2.5, 5 and 10 nM) suppressed the invasive and migratory ability of the MHCC97-H cells in a concentration-dependent manner, as assessed by the migration and invasion assay. The plots reveal the numbers of (C) migrated and (D) invaded cells at 24 h. *P<0.05 vs. 0 nM FK866. Scale bars, 50 μm.

(Fig. 4). These data suggest that FK866 treatment for 24 h results in a significant decrease in the invasive and migratory capabilities of MHCC97-H cells in a concentration-dependent manner compared with control cells.

FK866 inhibits the expression of SIRT1 and reverses the EMT in the HCC cell line MHCC97-H. Subsequently, the molecular mechanism underlying FK866-mediated inhibition of MHCC97-H cell invasion was investigated. SIRT1 participates in the EMT process of HCC, and E-cadherin and vimentin, as EMT markers, serve critical functions in cancer cell invasion (9,10). The results of the present study indicated that the expression of SIRT1 and vimentin was downregulated significantly and that of E-cadherin was upregulated significantly at the protein level by 10 nM FK866, as compared with the vehicle-treated control group (Fig. 5).

Discussion

HCC is one of the most common causes of malignant tumors, with a poor prognosis and a clinical 5-year postoperative recurrence rate of 70%, due primarily to high invasion and migration

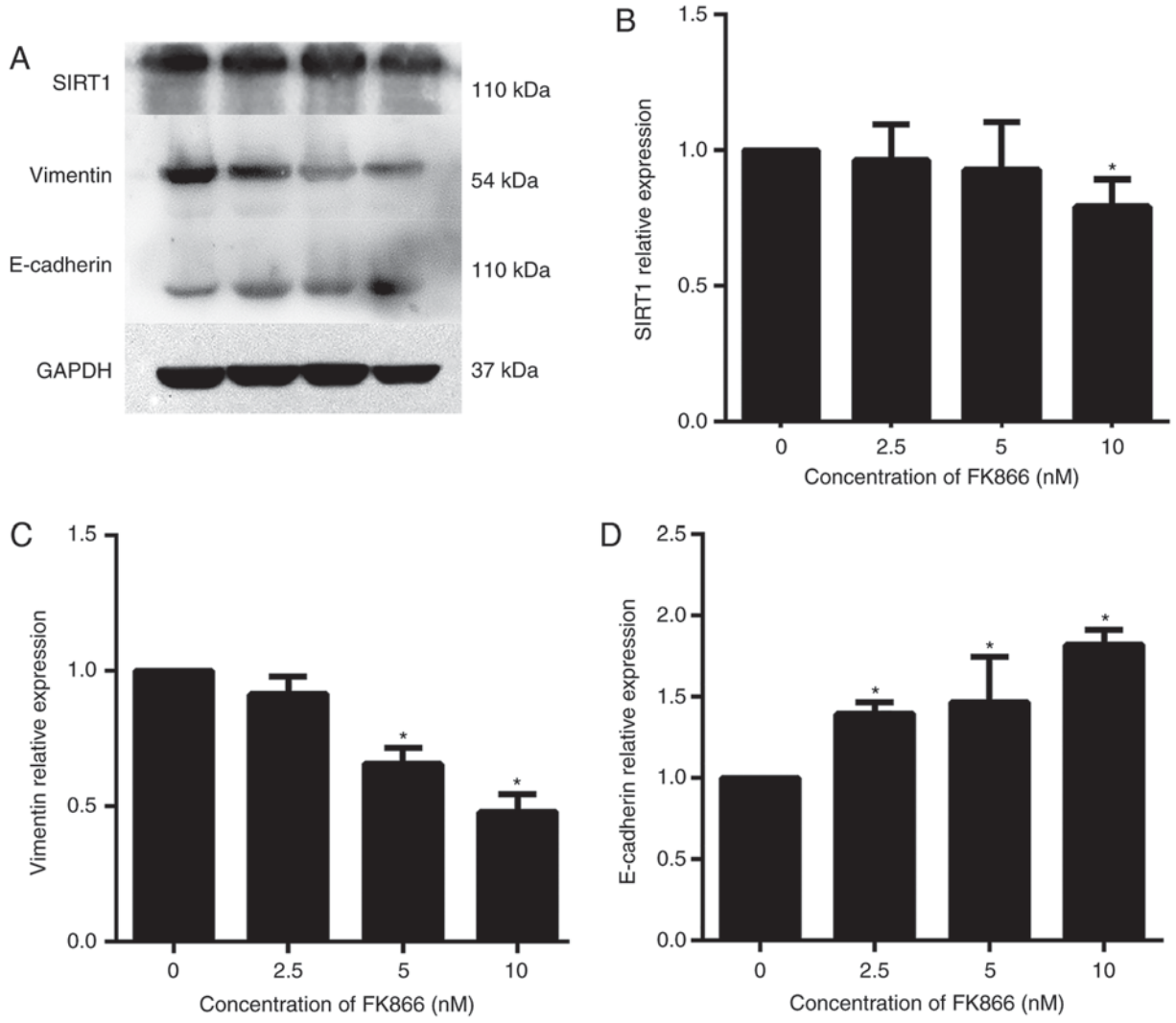

Figure 5. Effect of FK866 on the protein expression of SIRT1, E-cadherin and vimentin. FK866 inhibited the expression of SIRT1 at 10 nM concentration. SIRT1 inhibited the expression of vimentin at 5 and 10 nM, and promoted the expression of E-cadherin protein in MHCC97-H cells treated with 2.5, 5 and 10 nM FK866 for 24 h as compared with the control group (0 nM), (A) as measured by western blot analysis. Relative expression of (B) SIRT1, (C) vimentin and (D) E-cadherin in treated MHCC97-H cells compared with the untreated control. The data in the plots are expressed as the mean ± standard error of the mean of 5 replicates in 3 independent experiments. The protein expression levels were normalized to those of GAPDH. *P<0.05. SIRT1, silent information regulator 1; E-cadherin, epithelial cadherin.

rates of the HCC cells (1,2). HCC cell invasion and migration are two of the most clinically important characteristics of the tumor, and EMT serves a crucial function in these processes (3). Therefore, identifying potential novel targeted agents that are effective against EMT in HCC is an urgent requirement. In the present study, novel small-molecule NAMPT inhibitor FK866 was revealed to inhibit NAMPT/NAD^+/SIRT1-mediated EMT, suggesting that FK866 may be a novel targeted drug for the treatment of patients with metastatic HCC.

In normal and tumor cells, NAD^+ participates in several critical biological processes, including transcription, cell cycle progression, DNA repair, and circadian rhythm and metabolic regulation (22). NAD^+ is predominantly synthesized via the salvage pathway. NAMPT is the rate-limiting enzyme in the salvage pathway of NAD^+ and catalyzes the conversion of nicotinamide (a main precursor of NAD^+) into nicotinamide mononucleotide. The survival of the tumor cells requires more NAD^+ and NAMPT compared with that of the normal cells (23). One of the most important functions of NAD^+ is to act as an acetylation substrate of SIRT1, whose activity is directly regulated by the NAD^+ salvage pathway, in particular by the rate-limiting enzyme NAMPT (20). Consistent with these studies, the results of the present study revealed that inhibiting the expression of NAMPT suppresses the levels of NAD^+ and SIRT1. It has been identified previously that SIRT1 is associated with the EMT process of HCC (24). The level of SIRT1 increases in HCC, a phenomenon that is associated with poor prognosis in patients with HCC (25). SIRT1 also serves important functions in HCC stem cell self-renewal and promotes the invasiveness of tumor cells (25,26). E-cadherin and vimentin are EMT marker proteins that serve a central function in cancer cell invasion; SIRT1 is associated with the expression of invasive proteins in the tumor (9,10). SIRT1 is a critical regulator of cancer progression, by participating in HCC metastasis via EMT promotion (24). However, to the best of our knowledge, the precise molecular mechanism of how SIRT1 affects the invasion and metastasis of HCC cells has not yet been elucidated. In the present study, the function of SIRT1

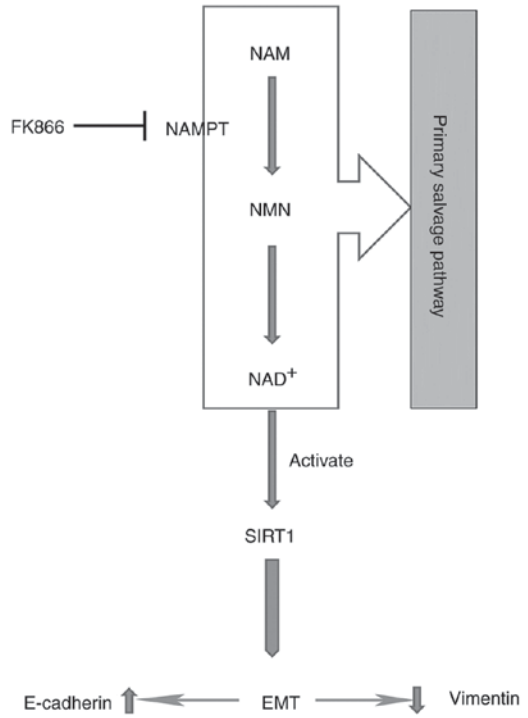

Figure 6. Function of FK866. In normal and tumor cells, NAD^+ is predominantly synthesized via the salvage pathway. NAMPT, as the rate-limiting enzyme in the salvage pathway of NAD^+, catalyzes the conversion of NAM (a main precursor substance of NAD^+) into NMN. One of the major functions of NAD^+ is an acetylation substrate of SIRT1, whose activity is directly regulated by the nicotinamide to NAD^+ salvage pathway, in particular the rate-limiting enzyme NAMPT. FK866, as the NAMPT inhibitor, inhibits the cell NAMPT/NAD^+/SIRT1 pathway and reverses the expression of EMT marker proteins, by upregulating E-cadherin and downregulating vimentin protein expression. NAD^+, nicotinamide adenine dinucleotide; NAMPT, nicotinamide phosphoribosyltransferase; NAM, nicotinamide; NMN, nicotinamide mononucleotide; SIRT1, silent information regulator 1; E-cadherin, epithelial cadherin; EMT, epithelial-mesenchymal transition.

in the EMT process of HCC cells was investigated using cell invasion and metastasis assays. Inhibiting the level of SIRT1 leads to the suppression the EMT, as demonstrated by the upregulation of E-cadherin and downregulation of vimentin. Furthermore, SIRT1 inhibits the EMT process by inhibiting the NAMPT/NAD^+ pathway.

Subsequently, the inhibitory regulation of the NAMPT/NAD^+/SIRIT1 pathway required further investigation. FK866, as an NAMPT inhibitor, significantly decreases the NAD^+ levels by inhibiting NAMPT; it also markedly inhibits the viability of different types of tumor cells (7,13-16). The results of the present study further confirm that FK866 decreases the levels of NAD^+ and ATP and suppresses the viability of HCC cells by inhibiting NAMPT in MHCC97-H cells.

FK866 has been used in a Phase II clinical trial as an antitumor drug (27). A recent study identified that FK866 provides a novel therapeutic strategy to enhance the efficacy of chemotherapeutic agents, including etoposide, against leukemia (28). Furthermore, FK866 also significantly enhances the antitumor activity of gemcitabine in pancreatic ductal adenocarcinoma cells and orthotopic xenograft mouse models, suggesting that FK866 may aid in overcoming gemcitabine resistance by decreasing the NAD^+ level and suppressing the glycolytic activity in pancreatic cancer treatment (29). However, the inhibitory effect of FK866 on tumor invasion and metastasis is rarely reported. In the present study, for the first time, the inhibitory function of the NAMPT-specific inhibitor FK866 in SIRT1-induced EMT in HCC was revealed, suggesting that FK866 may be used as a novel SIRT1 inhibitor. Regarding cell phenotype, these results indicated that FK866 inhibits MHCC97-H cell invasion and metastasis. In addition, FK866 decreases the SIRT1 protein expression and reverses that of EMT marker proteins; specifically, it upregulates E-cadherin and downregulates vimentin protein expression. The function of FK866 on EMT is demonstrated in a schematic diagram (Fig. 6).

In summary, NAMPT/NAD^+/SIRT1 is associated with energy metabolism in a number of downstream protein regulatory pathways that together comprise a systemic regulatory network in HCC cell invasion and migration.

The results of the present study confirm that FK866 significantly decreases the levels of NAD^+ and ATP, and suppresses the cell invasion and metastasis by inhibiting the NAMPT/NAD^+/SIRT1 signaling pathway in MHCC97-H cells. Overall, these results suggest that FK866 may be an effective targeted HCC drug and that the NAMPT/NAD^+/SIRT1 pathway may serve as a potential therapeutic alternative for HCC metastasis.

Acknowledgements

Not applicable.

Funding

The authors received grants from the National Natural Science Foundation of China (grant nos. 81773337 and 81401653) and the Natural Science Foundation of Shandong Province (grant no. ZR2015HL127), China.

Availability of data and materials

The datasets used and/or analyzed during the current study are available from the corresponding author on reasonable request.

Authors' contributions

BZ, GL, DS and SQ conceived and designed the experiments. BZ conducted all of the experiments. BZ wrote and revised the manuscript. XZ and WL analyzed the obtained data. All authors read and approved the final manuscript.

Ethics approval and consent to participate

Not applicable.

Patient consent for publication

Not applicable.

Competing interests

The authors declare that they have no competing interests.

References

1. Maluccio M and Covey A: Recent progress in understanding, diagnosing and treating hepatocellular carcinoma. CA Cancer J Clin 62: 394-399, 2012.
2. El-Serag HB: Hepatocellular carcinoma. N Engl J Med 365: 1118-1127, 2011.
3. Zhang Y, Wang W, Wang Y, Huang X, Zhang Z, Chen B, Xie W, Li S, Shen S and Peng B: NEK2 promotes hepatocellular carcinoma migration and invasion through modulation of the epithelial-mesenchymal transition. Oncol Rep 39: 1023-1033, 2018.
4. Liu T, Liu P Y and Marshall GM: The critical role of the class III histone deacetylase SIRT1 in cancer. Cancer Res 69: 1702-1705, 2009.
5. Jang KY, Noh SJ, Lehwald N, Tao GZ, Bellovin DI, Park HS, Moon WS, Felsher DW and Sylvester KG: SIRT1 and c-Myc promote liver tumor cell survival and predict poor survival of human hepatocellular carcinomas. PLoS One 7: e45119, 2012.
6. Bae HJ, Noh JH, Kim JK, Eun JW, Jung KH, Kim MG, Chang YG, Shen Q, Kim SJ, Park WS, *et al*: MicroRNA-29c functions as a tumor suppressor by direct targeting oncogenic SIRT1 in hepatocellular carcinoma. Oncogene 33: 2557-2567, 2014.
7. Liu G, Bi Y, Shen B, Yang H, Zhang Y, Wang X, Liu H, Lu Y, Liao J, Chen X, *et al*: SIRT1 limits the function and fate of myeloid-derived suppressor cells in tumors by orchestrating HIF-1α-dependent glycolysis. Cancer Res 74: 727-737, 2014.
8. Liang XJ, Finkel T, Shen DW, Yin JJ, Aszalos A and Gottesman MM: SIRT1 Contributes in part to cisplatin resistance in cancer cells by altering mitochondrial metabolism. Mol Cancer Res 6: 1499-1506, 2008.
9. Chen J, Zhang B, Wong N, Lo AW, To KF, Chan AW, Ng MH, Ho CY, Cheng SH, Lai PB, *et al*: Sirtuin 1 is upregulated in a subset of hepatocellular carcinomas where it is essential for telomere maintenance and tumor cell growth. Cancer Res 71: 4138-4149, 2011.
10. Hao C, Zhu PX, Yang X, Han ZP, Jiang JH, Zong C, Zhang XG, Liu WT, Zhao QD, Fan TT, *et al*: Overexpression of SIRT1 promotes metastasis through epithelial-mesenchymal transition in hepatocellular carcinoma. BMC Cancer 14: 978, 2014.
11. Lee Y, Drake AC, Thomas NO, Ferguson LG, Chappell PE and Shay KP: Dietary resveratrol increases mid-life fecundity of female Nothobranchius guentheri. Comp Biochem Physiol C Toxicol Pharmacol 208: 71-76, 2018.
12. Gerner RR, Klepsch V, Macheiner S, Arnhard K, Adolph TE, Grander C, Wieser V, Pfister A, Moser P, Hermann-Kleiter N, *et al*: NAD metabolism fuels human and mouse intestinal inflammation. Gut 67: 1813-1823, 2018.
13. Grubisha O, Smith BC and Denu JM: Small molecule regulation of Sir2 protein deacetylases. FEBS J 272: 4607-4616, 2005.
14. Schuster S, Penke M, Gorski T, Gebhardt R, Weiss TS, Kiess W and Garten A: FK866-induced NAMPT inhibition activates AMPK and downregulates mTOR signaling in hepatocarcinoma cell. Biochem Biophys Res Commun 458: 334-340, 2015.
15. Alaee M, Khaghani S, Behroozfar K, Hesari Z, Ghorbanhosseini SS and Nourbakhsh M: Inhibition of nicotinamide phosphoribosyltransferase induces apoptosis in estrogen receptor-positive MCF-7 breast cancer cells. J Breast Cancer 20: 20-26, 2017.
16. Mutz CN, Schwentner R, Aryee DNT, Bouchard EDJ, Mejia EM, Hatch GM, Kauer MO, Katschnig AM, Ban J, Garten A, *et al*: EWS-FLI1 confers exquisite sensitivity to NAMPT inhibition in Ewing sarcoma cells. Oncotarget 8: 24679-24693, 2017.
17. Liu HY, Li QR, Cheng XF, Wang GJ and Hao HP: NAMPT inhibition synergizes with NQO1-targeting agents in inducing apoptotic cell death in non-small cell lung cancer cells. Chin J Nat Med 14: 582-589, 2016.
18. Barraud M, Garnier J, Loncle C, Gayet O, Lequeue C, Vasseur S, Bian B, Duconseil P, Gilabert M, Bigonnet M, *et al*: A pancreatic ductal adenocarcinoma subpopulation is sensitive to FK866, an inhibitor of NAMPT. Oncotarget 7: 53783-53796, 2016.
19. Song TY, Yeh SL, Hu ML, Chen MY and Yang NC: A Nampt inhibitor FK866 mimics vitamin B3 deficiency by causing senescence of human fibroblastic Hs68 cells via attenuation of NAD(+)-SIRT1 signaling. Biogerontology 16: 789-800, 2015.
20. Imai S: Dissecting systemic control of metabolism and aging in the NAD World: The importance of SIRT1 and NAMPT-mediated NAD biosynthesis. FEBS Lett 585: 1657-1662, 2011.
21. Yang NC, Song TY, Chen MY and Hu ML: Effects of 2-deoxyglucose and dehydroepiandrosterone on intracellular NAD(+) level, SIRT1 activity and replicative lifespan of human Hs68 cells. Biogerontology 12: 527-536, 2011.
22. Chiarugi A, Dölle C, Felici R and Ziegler M: The NAD metabolome- a key determinant of cancer cell biology. Nat Rev Cancer 12: 741-752, 2012.
23. Bi TQ and Che XM: Nampt/PBEF/visfatin and cancer. Cancer Biol Ther 10: 119-125, 2010.
24. Choupani J, Mansoori Derakhshan S, Bayat S, Alivand MR and Shekari Khaniani M: Narrower insight to SIRT1 role in cancer: A potential therapeutic target to control epithelial-mesenchymal transition in cancer cells. J Cell Physiol 233: 4443-4457, 2018.
25. Liu L, Liu C, Zhang Q, Shen J, Zhang H, Shan J, Duan G, Guo D, Chen X, Cheng J, *et al*: SIRT1-mediated transcriptional regulation of SOX2 is important for self-renewal of liver cancer stem cells. Hepatology 64: 814-827, 2016.
26. Cheng J, Liu C, Liu L, Chen X, Shan J, Shen J, Zhu W and Qian C: MEK1 signaling promotes self-renewal and tumorigenicity of liver cancer stem cells via maintaining SIRT1 protein stabilization. Oncotarget 7: 20597-20611, 2016.
27. Esposito E, Impellizzeri D, Mazzon E, Fakhfouri G, Rahimian R, Travelli C, Tron GC, Genazzani AA and Cuzzocrea S: The NAMPT inhibitor FK866 reverts the damage in spinal cord injury. J Neuroinflammation 9: 66, 2012.
28. Grohmann T, Penke M, Petzold-Quinque S, Schuster S, Richter S, Kiess W and Garten A: Inhibition of NAMPT sensitizes MOLT4 leukemia cells for etoposide treatment through the SIRT2-p53 pathway. Leuk Res 69: 39-46, 2018.
29. Ju HQ, Zhuang ZN, Li H, Tian T, Lu YX, Fan XQ, Zhou HJ, Mo HY, Sheng H, Chiao PJ and Xu RH: Regulation of the Nampt-mediated NAD salvage pathway and its therapeutic implications in pancreatic cancer. Cancer Lett 379: 1-11, 2016.

This work is licensed under a Creative Commons Attribution-NonCommercial-NoDerivatives 4.0 International (CC BY-NC-ND 4.0) License.